ARTICLE

OBC
www.rsc.org/obc

# QM/MM calculations of kinetic isotope effects in the chorismate mutase active site

**Sergio Martí,[a] Vicent Moliner,*[a] Iñaki Tuñón*[b] and Ian H. Williams[c]**

[a] *Departament de Ciències Experimentals, Universitat Jaume I, Box 224, 12080 Castellón, SPAIN*

[b] *Departament de Química Física, Universitat de València, 46100 Burjassot, València, SPAIN*

[c] *Department of Chemistry, University of Bath, Bath BA2 7AY, United Kingdom*

***Received 28th October 2002, Accepted 16th December 2002***
***First published as an Advance Article on the web 17th January 2003***

Kinetic isotope effects have been computed for the Claisen rearrangement of chorismate to prephenate in aqueous solution and in the active site of chorismate mutase from *B. subtilus*. These included primary $^{13}C$ and $^{18}O$ and secondary $^{3}H$ effects for substitutions at the bond-making and bond-breaking positions. The initial structures of the putative stationary points on the potential energy surface, required for the calculations of isotope effects using the CAMVIB/CAMISO programs, have been selected from hybrid QM/MM molecular dynamical simulations using the DYNAMO program. Refinement of the reactant complex and transition-state structures has been carried out by means of AM1/CHARMM24/TIP3P calculations using the GRACE program, with full gradient relaxation of the position of >5200 atoms for the enzymic simulations, and with a box containing 711 water molecules for the corresponding reaction in aqueous solution. Comparison of these results, and of gas phase calculations, with experimental data has shown that the chemical rearrangement is largely rate-determining for the enzyme mechanism. Inclusion of the chorismate conformational pre-equilibrium step in the modelled kinetic scheme leads to better agreement between recent experimental data and theoretical predictions. These results provide new information on an important enzymatic transformation, and the key factors responsible for the kinetics of its molecular mechanism are clarified. Treatment of the enzyme and/or solvent environment by means of a large and flexible model is absolutely essential for prediction of kinetic isotope effects.

## 1 Introduction

Chorismate mutase catalyzes the rearrangement of chorismate to prephenate, a key step in the shikimate pathway for biosynthesis of the aromatic amino acids phenylalanine and tyrosine in bacteria, fungi and higher plants.[1,2] The fact that the shikimate pathway is not present in mammals makes this enzyme a suitable target for herbicides or anti-infective drugs.[3] Furthermore, it is one of the few examples of enzymes that catalyze a pericyclic reaction.[4] The concerted Claisen rearrangement (Scheme 1) proceeds through a chair-like transition state (TS) with asynchronous cleavage of a carbon–oxygen bond and formation of a carbon–carbon bond.[5,6] The rearrangement is preceded by a conformational equilibrium between diequatorial and diaxial forms of chorismate. The diequatorial structure is more populated in the gas phase, but the reaction proceeds from the diaxial conformer to the TS. The environment effect of solvent or enzyme changes the relative stability in favour the diaxial conformer.

A complete quantitative description of the enzyme-catalyzed mechanism would require determination of the rate constant for each of the individual steps along the reaction pathway, including substrate binding, enzyme conformational changes, chemical interconversion, and product release. However, in the absence of all of this information, useful insight into the catalytic action may nonetheless be provided by knowledge of geometrical and electronic properties of the TS in the active site. This can be derived by means of kinetic isotope effect (KIE) experiments but also from computational studies. Comparison of experimental and theoretical results provides a guide to the nature of the TS and the reaction mechanism, information that is necessary for the design of TS analogs as efficient inhibitors or as haptens for the selection of catalytic antibodies.[7]

The Claisen rearrangement of allyl phenyl ether was studied by McMichael and Korver,[8] who interpreted the secondary (2°) deuterium ($^{2}H$) KIEs to conclude that breakage of the C–O bond was more advanced than formation of the C–C bond in the TS. The asynchronous character of this rearrangement was also deduced by Gajewskii and Conrad[9] on the basis of 2° $^{2}H$ KIEs. Deuterium and heavy-atom KIEs were later measured by Shine, Saunders and co-workers for the rearrangements of allyl phenyl ether[10] and allyl vinyl ether,[11] who described a similar

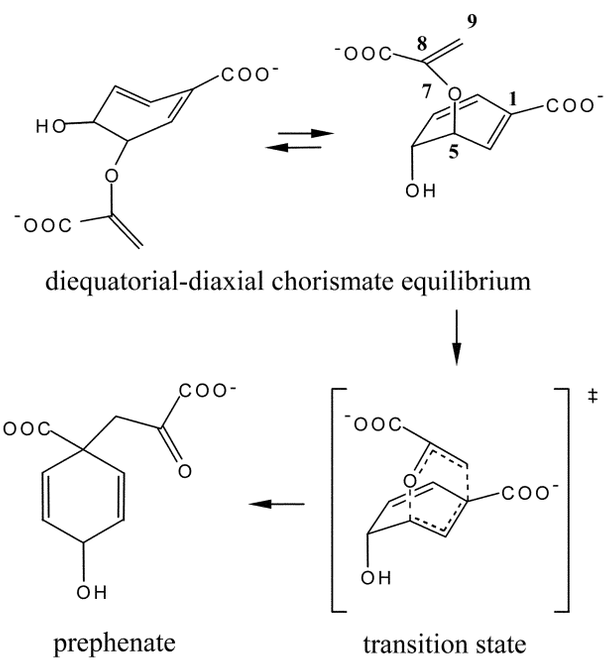


**Scheme 1** Rearrangement of chorismate to prephenate, preceded by its diequatorial to diaxial conformational equilibrium, and showing the atomic numbering.

DOI: 10.1039/b210508j

model for the TS. More recently, Singleton and coworkers[12] reinvestigated the KIEs for these rearrangements by means of a combined experimental and computational study.

Knowles and co-workers[13] were the first to study the effects of isotopic substitution upon the kinetics of the enzyme-catalyzed rearrangement of chorismate to prephenate. They employed a competitive method to measure the 2° tritium ($^3$H) KIEs for substitution at the bond-breaking (C9) and bond-making (C5) positions of $^{14}$C-labelled chorismate as the substrate for the chorismate mutase (EcCM) from *Escherichia coli*. Since this technique evaluates the isotope effect on $V_{max}/K_m$, it would provide information about the changes of hybridization at C5 and C9 occurring between free chorismate in solution and the TS for the rate-limiting step of the catalyzed reaction. However, the measured values of $k_H/k_T$ at pH 7.5 and 30 °C were unity within experimental error at both positions; this was interpreted as indicating that the rate-limiting TS occurred before the rearrangement itself. Subsequently a 2° $^3$H KIE of 0.96 for substitution at the C–4 position of chorismate, and a solvent $^2$H KIE of 2.23, were also measured by Knowles and co-workers for the reaction catalyzed by the same enzyme.[14] They suggested that the available evidence was consistent with a mechanism in which rate-limiting heterolytic cleavage of the C5–O7 bond of chorismate was assisted by attack of an enzymic nucleophile at C5.

Cleland, Hilvert and co-workers[15] have more recently measured heavy-atom KIEs on the reaction catalyzed by the chorismate mutase (BsCM) from wild-type *Bacillus subtilis* and by the viscosity-insensitive C75S variant, using a sensitive remote label method. They used chorismate substituted with $^{13}$C at the C1 position, the site of bond formation, and with $^{18}$O at the O7 position, the site of bond cleavage. Their observation of significant heavy-atom effects showed that, contrary to the earlier studies on EcCM, the chemical rearrangement was largely rate determining with BsCM and that the enzymatic TS was highly polarized. They noted that, since the chemistry was unlikely to be fully rate-limiting even for this enzyme, their experimental KIEs should be considered as minimum values. They also carried out gas-phase density functional theory (DFT) KIE calculations, obtaining a smaller $^{18}$O effect and a larger $^{13}$C effect than observed for the enzymatic reaction; suggesting that the TS might be more dissociative for the enzymatic reaction than for the uncatalyzed reaction in solution.

As part of a continuing theoretical study of the chorismate–prephenate rearrangement mechanism of chorismate mutase,[16] in this paper we present results obtained by use of a fully flexible hybrid quantum-mechanical/molecular-mechanical (QM/MM) method. To our knowledge, this is the first time that KIE calculations based on a QM/MM approach have been performed for the chorismate to prephenate rearrangement in the BsCM active site with good agreement between theoretical and experimental data. QM/MM methods are based on the concept introduced by Warshel and Levitt in 1976.[17] Previous studies using this methodology have been restricted to partial geometry optimizations following gas-phase reaction paths or to approximate strategies (*e.g.* freezing the MM part of the system). From TS and reactant–complex (R) structures located and characterized in the enzyme environment we have obtained heavy-atom KIEs much closer to the experimental data than the ones reported previously in the literature.

## 2 Computational methods

Gas-phase calculations were carried out with the AM1[18] semi-empirical molecular orbital method and the B3LYP/6–31G* level[19] of DFT using the GAUSSIAN98 package of programs.[20] Minima and first-order saddle points were located using the Berny algorithm[21] and were characterized by inspection of the analytical Hessian matrix, which in the case of a TS has a single negative eigenvalue.

QM/MM calculations in solution were carried out using the CHARMM24b2[22] and GRACE[23] programs. The reacting system was treated by AM1, placed in a cavity deleted from a 28 Å cubic box of 711 water molecules described by non-rigid TIP3P empirical potentials. A solvent boundary potential was employed to prevent evaporation of water molecules from the surface of the box during the optimisations.

For the QM/MM enzyme calculations the structure for BsCM was obtained from the Protein Data Bank.[24] In these calculations, carried out using CHARMM24b2 and GRACE, the QM subsystem was the chorismate, while the enzyme trimer plus crystallization and solvation water molecules formed the MM subsystem (5654 enzyme atoms plus 3835 non-rigid TIP3P water molecules). The resulting enzymatic system was a 58 Å cubic box (17183 atoms in total). During the enzyme optimizations the QM atoms and the MM atoms lying in a sphere of 20 Å radius centered on the QM system were allowed to move (a total of 5234 atoms).

QM/MM stationary-point location and characterization were guided by means of GRACE, which uses a Newton–Raphson algorithm. In this method, the system is divided into two parts, the core and the environment. The Hessian matrix is calculated explicitly only for those atoms belonging to the core. Once this partitioning has been done, the stationary point (minimum or saddle point) location is carried out in the degrees of freedom of the core. Before each energy and gradient evaluation step for the core, the degrees of freedom of the environment are relaxed to maintain an approximately zero gradient and to minimise the potential energy. The core region contained all 24 QM atoms, thus giving a Hessian matrix of order 72. The intrinsic reaction coordinate (IRC) paths were traced down to the reactant and product valleys from each saddle point, as previously described,[23b] followed by an optimization of the full system. The IRC calculations employed a modified version of the MOPAC routine based on the method of Gordon and coworkers.[25] The initial step was taken in the direction of the transition vector from diagonalisation of the mass-weighted Hessian. Subsequent steps along the IRC utilized the gradient vector for the QM atoms computed with full relaxation of the MM atoms; the difference between this and the true IRC using the full gradient vector is trivial since the contribution from atoms outside the core is negligible. It was essential to use a small step size in the IRC computation in order to allow the environment to relax at every single step and then to prevent the algorithm halting falsely.

Once the potential energy profiles were obtained in the condensed phase (both aqueous and enzymatic media), the potentials of mean force (PMF)[26] were calculated using the weighted histogram analysis method (WHAM)[27] combined with the umbrella-sampling approach as implemented in the DYNAMO program.[28] The condensed-phase systems were the same as those described above (cubic boxes with sides of 28 Å and 58 Å for solution and enzyme phases, respectively). Periodic boundary conditions were used in both cases. The starting geometries were the saddle-point structures previously located in the two different environments, while the distinguished reaction coordinate was taken as the antisymmetric combination of the distances describing the breaking and forming bonds, *i.e.* $d_{CC} - d_{CO}$ (see Scheme 1). This variable represents very closely (or exactly) the IRCs that were found in the enzyme, in the gas phase and in solution and so it was the natural choice for determining the PMFs. The procedure for the PMF calculation was straightforward and required a series of molecular dynamics simulations in which the reaction coordinate variables were constrained about particular values. The values of the variables sampled during the simulations were then pieced together to construct a distribution function from which the PMF was obtained. These free energy profiles, as well as a discussion of geometries and energetics, are reported elsewhere.[16d] The technical details of the approach are very similar to those employed

previously[29] and so are not repeated here. A temperature of 300 K was employed throughout this work using the canonical thermodynamical ensemble (NVT).

The rigid-rotor/harmonic-oscillator approximations were used with the CAMVIB/CAMISO programs[30] to calculate the KIEs. Gas-phase results were obtained by computing the full Hessian, while QM/MM KIEs were calculated by using either a small core of 24 atoms (equivalent to the QM region) or else a large core comprising 66 atoms in solution or 67 atoms in the enzyme (Fig. 1). The R and TS structures used to compute

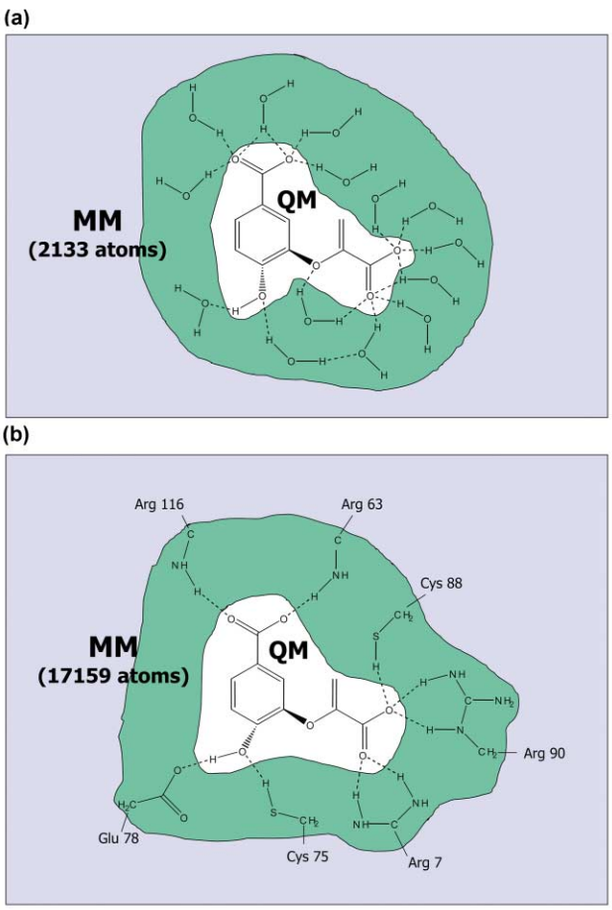


**Fig. 1** Chorismate in (a) aqueous solution and (b) the active site of *B. subtilis* chorismate mutase. The QM region is shown against a white background; the blue region contains the MM atoms excluded from all Hessian calculations, while the green region contains the MM atoms included (along with the QM atoms) in the "large-core" Hessian calculations but excluded from the "small-core" calculations.

the QM/MM KIEs were selected as the ones closest to the averages obtained in their respective windows of the PMF (from ref. 16*d*); these selected structures were subsequently fully optimised to minima and saddle points, respectively, using CHARMM and GRACE. In common with other vibrational properties such as IR spectroscopic frequencies, isotope effects are local properties,[31] in the sense that they are determined by the immediate environment of the center of isotopic substitution; this local environment extends only by one or two bond distances (″cut-off-rule″). This justifies the fact that the ratios of partition functions were calculated not for the whole enzyme, but only for a subset of the full system. Furthermore, as pointed out by Singleton and co-workers,[12] due to the fact that entropy and ZPE effects on the TS geometry should be minimal, the Claisen rearrangement is a relatively good case for application of the semiclassical approximation for calculation of isotope effects. All force constants and vibrational frequencies were used without scaling in these calculations.

**Table 1** Selected interatomic distances (Å) for the gas phase optimized geometries of the transition state in the gas phase (from ref. 16*a*) and average values of transition state structures obtained with DYNAMO QM/MM statistical calculations in condensed media; aqueous solution and enzyme environment (from ref. 16*d*)

| | Gas phase | | | | Condensed media | |
|---|---|---|---|---|---|---|
| | AM1 | | B3LYP/6–31G* | | AM1/MM | |
| | $OH_{in}$ | $OH_{out}$ | $OH_{in}$ | $OH_{out}$ | water | BsCM |
| C5 ··· O7 | 1.8239 | 1.8537 | 2.1003 | 2.2749 | 1.831 | 1.971 |
| C1 ··· C9 | 2.1195 | 2.1640 | 2.5734 | 2.7188 | 2.141 | 2.218 |

**Table 2** Gas phase secondary tritium kinetic isotope effects ($k_H/k_T$) and primary heavy atom kinetic isotope effects ($k_{12C}/k_{13C}$ and $k_{16O}/k_{18O}$) for the chorismate to prephenate rearrangement. The isotope substitutions have been done on $OH_{in}$ and $OH_{out}$ chorismate conformers. The tritium labels have been done on carbon 5 [5-$^3$H] and carbon 9 [9-$^3$H] positions, following the numbering depicted in Scheme 1

| | AM1 | | B3LYP/6–31G* | |
|---|---|---|---|---|
| | $OH_{in}$ | $OH_{out}$ | $OH_{in}$ | $OH_{out}$ |
| [5-$^3$H] $k_H/k_T$ | 1.1237 | 1.0693 | 1.2638 | 1.3326 |
| [9-$^3$H] $k_H/k_T$ | 0.8358 | 0.8377 | 0.9497 | 1.0030 |
| $k_{12C}/k_{13C}$ | 1.0191 | 1.0176 | 1.0145 | 1.0149 |
| $k_{16O}/k_{18O}$ | 1.0502 | 1.0519 | 1.0387 | 1.0416 |

## 3 Results and discussion

Selected interatomic distances for the gas-phase optimized geometries of two conformations of the TS ($OH_{in}$ and $OH_{out}$, considering the relative position of the hydroxy group with respect to the ring, as described in ref. 16*a*), are presented in Table 1. The orientation of the hydroxy group introduces important changes in the TS: the $OH_{out}$ structure is more dissociative than the $OH_{in}$. It is also important to indicate that the latter TS is lower in energy, but the $OH_{out}$ reaction path is the one having the lower energy barrier.[16a] Average values of C5–O7 and C1–C9 distances in the TSs obtained by means of QM/MM statistical calculations with DYNAMO are also listed in Table 1. Note that $OH_{in}$ and $OH_{out}$ are not distinguished for the solution-phase structures, as the hydroxy-group orientation appears to be quite flexible. In contrast, in the enzyme the $OH_{out}$ is preferred with respect to the $OH_{in}$ due to specific substrate–protein interactions.

Both AM1 and B3LYP predict a chair-like TS in the gas phase. However, as previously reported by Singleton and co-workers,[12] the AM1 structure has 1,4-diyl electronic character, while B3LYP gives a more dissociative bisallyl-like structure. The TS obtained in solution is slightly compressed relative to the enzymatic TS: both C5–O7 and C1–C9 distances are shorter in solution than in the enzyme.

In order to assess the suitability of the AM1 method for studying this Claisen rearrangement, we have performed (following Lyne *et al.*[32]) gas-phase KIE calculations using both this and a DFT method. While AM1 has been extensively applied in the past to study gas-phase pericyclic reactions with varying degrees of success,[33] B3LYP/6–31G* calculations have yielded isotope effects for a number of reactions in excellent agreement with experiment.[34] Table 2 lists 2° $^3$H KIEs ($k_H/k_T$), for tritium substitution on C5 and C9 positions, and heavy-atom KIEs ($k_{12C}/k_{13C}$ for substitution at C1 and $k_{16O}/k_{18O}$ for substitution at O7) for the chorismate to prephenate rearrangement.

The calculated gas-phase heavy-atom KIEs are in the normal direction ($k_{light} > k_{heavy}$) but are slightly smaller with B3LYP than with AM1. This accords with the computed TS structures: longer C5–O7 and C1–C9 distances with B3LYP imply smaller bond stretching force constants and, consequently, smaller

**Table 3** Tritium ($k_H/k_T$) and heavy atom kinetic isotope effects ($k_{12C}/k_{13C}$ and $k_{16O}/k_{18O}$) calculated (a) in aqueous solution and (b) in enzymatic environment for the chorismate to prephenate rearrangement. Two sub-sets of atoms have been used for the hessian calculation: *small core* (24 atoms) and *large core* (67 and 66 atoms for solution and enzyme calculations, respectively). Experimental tritium KIE were obtained from ref 13 while heavy atom KIE were obtained from ref 15

| | QM/MM calculations | | |
|---|---|---|---|
| (a) | Small core | Large core | Experimental |
| [5-$^3$H] $k_H/k_T$ | 1.1196 | 1.1435 | 1.149 ± 0.012 |
| [9-$^3$H] $k_H/k_T$ | 0.8988 | 0.9215 | 0.992 ± 0.012 |
| | QM/MM calculations | | |
| (b) | Small core | Large core | Experimental |
| [5-$^3$H] $k_H/k_T$ | 1.1456 | 1.1471 | 1.003 ± 0.020 |
| [9-$^3$H] $k_H/k_T$ | 0.8515 | 0.8598 | 1.012 ± 0.004 |
| $k_{12C}/k_{13C}$ | 1.0186 | 1.0179 | 1.0043 ± 0.0002 |
| $k_{16O}/k_{18O}$ | 1.0476 | 1.0481 | 1.045 ± 0.003 |

primary KIEs. The shorter C5–O7 distance for the breaking bond with AM1 than with B3LYP implies less rehybridisation at C5 in the TS, and smaller (closer to unity) normal values of the 2° $^3$H KIEs for tritium substitution at this [C5–$^3$H] position. Similarly, the shorter C1–C9 distance for the forming bond with AM1 than with B3LYP implies more rehybridisation at C9 in the TS, and larger (further from unity) inverse values of the 2° $^3$H KIEs for tritium substitution at the [9-$^3$H] position.

The second stage in our study was to compute these KIEs in the presence of aqueous and enzyme environments in order to carry out a direct comparison between theoretical and experimental data. Table 3 lists the 2° $^3$H and 1° heavy-atom KIEs calculated by means of the QM/MM procedure described in the previous section, together with experimental results of Addadi *et al.*[13] and Gustin *et al.*[15]. However, we note that the 2° $^3$H KIEs reported by Addadi *et al.* were obtained with EcCM and not with BsCM. In the former, chorismate mutase is a single domain of the bifunctional enzyme prephenate dehydratase with a low percentage sequence identity with respect to the BsCM domain, used in our calculations.

If we accept that KIEs reflect changes in local bonding characteristics, and that solvent–solute and enzyme–substrate hydrogen-bonding interactions may affect force constants for solute/substrate atoms, then it follows that these interactions may also lead to changes in isotopic fractionation factors as between R and TS. The 2 $^3$H KIEs calculated for aqueous solution (Table 3a) using only a small core are in qualitative agreement with experiment, but significantly better agreement is obtained when the large core is used, which includes neighbouring solvent molecules. In contrast, the 2 $^3$H KIEs calculated for the enzyme environment (Table 3b) do not agree with the experimental values.

If we focus our attention on the heavy-atom KIEs presented in Table 3b, we see that the calculated $k_{16O}/k_{18O}$ results (small-core 1.0476 and large-core 1.0481) agree quite well with the experimental value of 1.045 ± 0.003 reported by Gustin *et al.*,[15] whereas a larger discrepancy is found between the calculated $k_{12C}/k_{13C}$ results (small-core 1.0186 and large-core 1.0179) and the experimental value of 1.0043 ± 0.0002. Increasing the size of the Hessian to include immediate enzyme–substrate interactions in these calculations for the enzymic environment again leads to a small improvement in the calculated result, but the effect is not dramatic. Nonetheless, considering all the aqueous solution (Table 3a) and enzymic (Table 3b) results, calculated KIEs are improved with respect to experiment by increasing the size of the core.

Table 4 contains the results of our attempt to improve the theoretical model by taking account of the substrate binding

**Table 4** Tritium ($k_H/k_T$) and heavy atom kinetic isotope effects ($k_{12C}/k_{13C}$ and $k_{16O}/k_{18O}$) calculated for the chorismate to prephenate rearrangement as a product of $KIE_{obs} = EIE_1 \times KIE_2$, (see the text for details). Experimental KIE obtained from ref 13 and ref 15 for the $k_H/k_T$ and the heavy atom KIEs, respectively

| | $EIE_1$ | $KIE_2$ | $KIE_{obs}$ | Experimental |
|---|---|---|---|---|
| [5-$^3$H] $k_H/k_T$ | 0.9889 | 1.1456 | 1.1329 | 1.003 ± 0.020 |
| [9-$^3$H] $k_H/k_T$ | 1.0436 | 0.8515 | 0.8886 | 1.012 ± 0.004 |
| $k_{12C}/k_{13C}$ | 1.0006 | 1.0186 | 1.0192 | 1.0043 ± 0.0002 |
| $k_{16O}/k_{18O}$ | 1.0032 | 1.0476 | 1.0509 | 1.045 ± 0.003 |

equilibrium. As demonstrated previously,[16d,e] the pseudodiaxial chorismate conformer is the most stable reactant-like structure (and also the one from which reaction occurs) both in water and in the enzyme. Consequently we propose that the observed KIE could be the product of the equilibrium isotope effect upon binding of chorismate from aqueous solution to the enzyme and the KIE for the rearrangement within the enzyme active site, according to the following simple kinetic scheme:

$$\text{(diaxial-chorismate)}_{water} \underset{k_{-1}}{\overset{k_1}{\rightleftharpoons}} \text{(diaxial-chorismate)}_{enzyme} \xrightarrow{k_2} \text{(prephenate)}_{enzyme}$$

$$KIE_{obs} = EIE_1 \times KIE_2$$

As seen from Table 4, inclusion of this pre-equilibrium step improves all the calculated KIEs with respect to experiment, except the $k_{12C}/k_{13C}$ result, for which the calculated EIE is in any case almost null.

Our use of the AM1 method for the QM region of the QM/MM calculations reported in this paper is dictated by practical reasons that are further underlined by the observations that better KIE results are obtained by inclusion of larger numbers of atoms in the Hessian calculations and by consideration of the pre-equilibrium binding step. However, the differences between the AM1 and B3LYP/6–31G* results in Table 2 clearly suggest that use of the DFT method would in every case probably lead to a calculated KIE value closer to experiment than the AM1 result. QM/MM calculations where the quantum region was treated with a DFT method would render more dissociative bisallyl-like TS structures with frequencies closer to experimental data than the ones obtained with a semiempirical AM1 method. This prediction arises from our comparison of gas phase AM1 and B3LYP/6–31G* calculations but is also supported, in part, from recent QM/MM calculations of Lee *et al.* on this enzyme reaction.[35] Using a Hartree–Fock wave function to describe prephenate, the authors obtained a TS with an almost complete broken C5–O7 ether bond and a C1–C9 bond distance significantly larger than the one obtained by us.

## Concluding remarks

We have for the first time calculated KIEs for the chorismate conversion to prephenate in aqueous solution and in the BsCM active site by means of hybrid QM/MM methods. Secondary tritium and primary $^{13}$C and $^{18}$O KIEs at the positions of bond-making and bond-breaking have been predicted with varying degrees of agreement with experiments. The results may be summarized as follows:

(i) Provided that the partition functions for R and TS include some force constants associated with water molecules surrounding the solute, 2° $^3$H KIEs obtained in solution agree well with the experimental results of Addadi *et al.*[13]

(ii) However, 2° $^3$H KIEs calculated for reaction in the enzyme environment do not fit with the experimental results of Addadi *et al.*[13]. This discrepancy may arise from the fact that our calculations are for BsCM whereas the experimental data

were obtained using EcCM, the enzyme from a different organism.

(iii) The primary $k_{16O}/k_{18O}$ KIE calculated for substitution at O7 agrees reasonably well with the experimental value of Gustin *et al.*[15] provided that the pre-equilibrium step is included.

(iv) The primary $k_{12C}/k_{13C}$ KIE calculated for substitution at C1 is not in agreement with the experimental value. The results in Tables 1 and 2 clearly show that AM1 predicts a TS with C1–C9 distance considerably shorter than that predicted by B3LYP (*cf.* refs. 12 and 31), and this fact may account for the overestimation of the KIE. However, it is worth noting here that a lack of agreement may be due either to deficiencies in the calculations or to uncertainties and/or inaccuracies in the experimental determination. Singleton and co-workers stressed this point in their recent study of Claisen and aromatic Claisen rearrangements.[12] Finally, the discrepancy could arise because, as suggested by Mattei *et al.*,[36] BsCM is partially diffusion controlled and the rearrangement TS is therefore not completely rate limiting.

## Acknowledgements

We are indebted to DGI for project DGI BQU2000-C03, BANCAIXA for project P1A99-03 and Generalitat Valenciana for project GV01-324, which supported this research, and the Servei d'Informatica of the Universitat Jaume I for providing us with computer capabilities. S. M. thanks UJI-BANCAIXA Foundation for a post-doctoral fellowship.

## References

1 E. Haslam, *Shikimic Acid: Metabolism and Metabolites*, John Wiley & Sons, New York, 1993.
2 U. Weiss, J. M. Edwards, *The Biosynthesis of Aromatic Compounds*, Wiley, New York, 1980.
3 T. Fitzpatrick, S. Ricken, M. Lanzer, N. Amrhein, P. Macheroux and B. Kappes, *Mol. Biol.*, 2001, **40**, 65.
4 E. M. Dirggers, H. S. Cho, C. W. Liu, C. P. Katzka, A. C. Braisted, H. D. Ulrich, D. E. Wemmer and P. G. Schultz, *J. Am. Chem. Soc.*, 1998, **120**, 1945.
5 S. G. Sogo, T. S. Widlanski, J. H. Hoare, C. E. Grimshaw, G. A. Berchtold and J. R. Knowles, *J. Am. Chem. Soc.*, 1984, **106**, 2701.
6 S. D. Copley and J. R. Knowles, *J. Am. Chem. Soc.*, 1987, **109**, 5008.
7 I. H. Williams, *Chem. Soc. Rev.*, 1993, **22**, 277.
8 K. D. McMichael and G. L. Korver, *J. Am. Chem. Soc.*, 1979, **101**, 2746.
9 J. J. Gajewski and N. D. Conrad, *J. Am. Chem. Soc.*, 1979, **101**, 2747.
10 (*a*) L. Kupczyk-Subotkowska, W. H. Saunders and H. J. Shine, *J. Am. Chem. Soc.*, 1988, **110**, 7153; (*b*) L. Kupczyk-Subotkowska, W. Subotkowski, W. H. Saunders and H. J. Shine, *J. Am. Chem. Soc.*, 1992, **114**, 3441.
11 L. Kupczyk-Subotkowska, W. H. Saunders, H. J. Shine and W. Subotkowski, *J. Am. Chem. Soc.*, 1993, **115**, 5957.
12 M. P. Meyer, A. J. DelMonte and D. A. Singleton, *J. Am. Chem. Soc.*, 1999, **121**, 10865.
13 L. Addadi, E. K. Jaffe and J. R. Knowles, *Biochemistry*, 1983, **22**, 4494.
14 W. J. Guilford, S. D. Copley and J. R. Knowles, *J. Am. Chem. Soc.*, 1987, **109**, 5013.
15 D. J. Gustin, P. Mattei, P. Kast, O. Wiest, L. Lee, W. W. Cleland and D. Hilvert, *J. Am. Chem. Soc.*, 1999, **121**, 1756.
16 (*a*) S. Martí, J. Andrés, V. Moliner, E. Silla, I. Tuñón and J. Bertrán, *Theor. Chem.*, 2001, **105**, 207; (*b*) S. Martí, J. Andrés, V. Moliner, E. Silla, I. Tuñón and J. Bertrán, *J. Phys. Chem. B.*, 2000, **104**, 11308; (*c*) S. Martí, J. Andrés, V. Moliner, E. Silla, I. Tuñón, J. Bertrán and M. J. Field, *J. Am. Chem. Soc.*, 2001, **123**, 1709; (*d*) S. Martí, J. Andrés, V. Moliner, E. Silla, I. Tuñón, J. Bertrán, *Chem. Eur. J.*, 2002, in press; (*e*) S. Martí, J. Andrés, V. Moliner, E. Silla, I. Tuñón, J. Bertrán, *Theochem.*, 2002, in press.
17 A. Warshel and M. Levitt, *J. Mol. Biol.*, 1976, **103**, 227.
18 M. J. S. Dewar, E. G. Zoebisch, E. F. Healy and J. J. P. Stewart, *J. Am. Chem. Soc.*, 1985, **107**, 3902.
19 (*a*) A. D. Becke, *Phys. Rev. A*, 1988, **38**, 3098; A. D. Becke, *J. Chem. Phys.*, 1993, **98**, 5648; (*b*) C. Lee, W. Yang and R. G. Parr, *Phys. Rev. B*, 1988, **37**, 785; (*c*) P. J. Stevens, J. F. Devlin, C. F. Chabalowski and M. J. Frisch, *J. Phys. Chem.*, 1994, **98**, 11623.
20 M. J. Frisch, G. W. Trucks, H. B. Schlegel, G. E. Scuseria, M. A. Robb, J. R. Cheeseman, V. G. Zakrzewski, J. A. Montgomery Jr., R. E. Stratmann, J. C. Burant, S. Dapprich, J. M. Millam, A. D. Daniels, K. N. Kudin, M. C. Strain, O. Farkas, J. Tomasi, V. Barone, M. Cossi, R. Cammi, B. Mennucci, C. Pomelli, C. Adamo, S. Clifford, J. Ochterski, G. A. Petersson, P. Y. Ayala, Q. Cui, K. Morokuma, D. K. Malick, A. D. Rabuck, K. Raghavachari, J. B. Foresman, J. Cioslowski, J. V. Ortiz, B. B. Stefanov, G. Liu, A. Liashenko, P. Piskorz, I. Komaromi, R. Gomperts, R. L. Martin, D. J. Fox, T. Keith, M. A. Al-Laham, C. P. Peng, A. Nanayakkara, C. Gonzalez, M. Challacombe, P. M. W. Gill, B. Johnson, W. Chen, M. W. Wong, J. L. Andres, C. Gonzalez, M. Head-Gordon, E. S. Replogle, J. A. Pople, Gaussian 98, Revision A.6, Gaussian, Inc., Pittsburgh PA, 1998.
21 H. B. Schlegel, *J. Comput. Chem.*, 1982, **3**, 214.
22 B. R. Brooks, R. E. Bruccoleri, B. D. Olafson, D. J. States, S. Swaminathan and M. Karplus, *J. Comput. Chem.*, 1983, **4**, 187.
23 (*a*) V. Moliner, A. J. Turner and I. H. Williams, *Chem. Commun.*, 1997, 1271; (*b*) A. J. Turner, V. Moliner and I. H. Williams, *Phys. Chem. Chem. Phys.*, 1999, **1**, 1323.
24 Y. M. Chook, H. Ke and W. N. Lipscomb, *Proc. Natl. Acad. Sci. USA*, 1993, **90**, 8600. Protein Data Bank ID code 1COM.
25 (*a*) M. W. Schmidt, M. S. Gordon and M. Dupuis, *J. Am. Chem. Soc.*, 1985, **107**, 1585; (*b*) J. J. P. Stewart, MOPAC 7 (QCPE 457), *QCPE Bull.*, 1993, **13**, 42.
26 B. Roux, *Comput. Phys. Commun.*, 1995, **91**, 275.
27 G. M. Torrie and J. P. Valleau, *J. Comput. Phys.*, 1977, **23**, 187.
28 M. J. Field, M. Albe, C. Bret, F. Proust de Martin and A. Thomas, *J. Comput. Chem.*, 2000, **21**, 1088.
29 F. Proust de Martin, R. Dumas and M. J. Field, *J. Am. Chem. Soc.*, 2000, **122**, 7688.
30 (*a*) I. H. Williams, *Chem. Phys. Lett.*, 1982, **88**, 462; (*b*) I. H. Williams, *J. Mol. Struct. THEOCHEM*, 1983, **11**, 275.
31 J. Sühnel, R. L. Schowen, in *Enzyme Mechanism from Isotope Effects*, ed. P. F. Cook, CRC Press, Boca Raton, 1991.
32 P. D. Lyne, A. J. Mulholland and W. G. Richards, *J. Am. Chem. Soc.*, 1995, **117**, 11345.
33 K. N. Houk, J. Gonzalez and Y. Li, *Acc. Chem. Res.*, 1995, **28**, 81.
34 (*a*) B. R. Beno, K. N. Houk and D. A. Singleton, *J. Am. Chem. Soc.*, 1996, **118**, 9984; (*b*) D. A. Singleton, S. L. Merrigan, J. Liu and K. N. Houk, *J. Am. Chem. Soc.*, 1997, **119**, 3385; (*c*) A. J. Del Monte, J. Haller, K. N. Houk, K. B. Sharpless, D. A. Singleton, T. Strassner and A. A. Thomas, *J. Am. Chem. Soc.*, 1997, **119**, 9907.
35 Y. S. Lee, S. E. Worthington, M. Krauss and B. R. Brooks, *J. Phys. Chem. B*, 2002, **106**, 12059.
36 P. Matthei, P. Kast and D. Hilvert, *Eur. J. Biochem.*, 1999, **261**, 25.